RUHR-UNIVERSITÄT BOCHUM
Institute of Geology, Mineralogy and Geophysics

Earthquake source parameter analysis shows hydraulic fracturing induced events are consistent with fault reactivation under regional stress in northeastern British Columbia, Canada

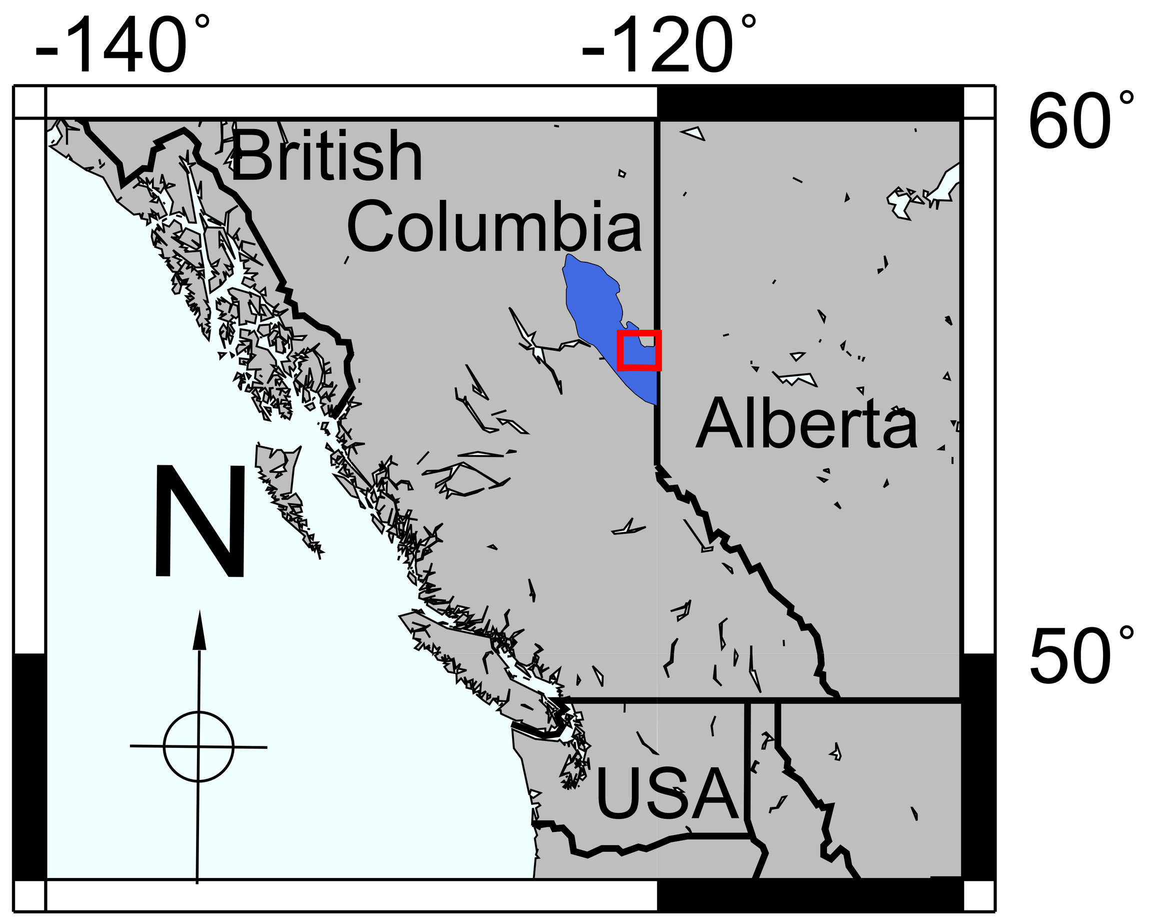

Marco P. Roth[1], Alessandro Verdecchia[1,2], Kilian B. Kemna[1], John Onwuemeka[2], Rebecca M. Harrington[1], and Yajing Liu[2]

[1]Ruhr University Bochum, Bochum, Germany
[2]McGill University, Montreal, QC, Canada

The work presented here is based on a manuscript in revision for Seismological Research Letters.
Roth, M.P., Verdecchia, A., Harrington, R.M., And Liu, Y. (2020): High-resolution imaging of hydraulic fracturing induced earthquake clusters in the Dawson-Septimus area, northeast British Columbia, Canada.

Motivation

- In the last decade, Western Canada Sedimentary Basin (WCSB) experienced a large number of earthquakes induced by hydraulic fracturing (HF)
- The Montney Basin has hosted the largest HF-induced earthquakes in Canada, including a M_L 4.5 on 11/30/2018 near Dawson Creek and a M_w 4.6 on 08/17/2015 near Fort St. John, as well as several M3+ earthquakes close to Dawson Creek.

Objectives

- Build a detailed earthquake catalog using data of stations from Ruhr University Bochum (RUB), McGill University, and Natural Resources Canada (NRCan).
- Investigate the spatial and temporal correlation between earthquake occurrence and HF injection activity.

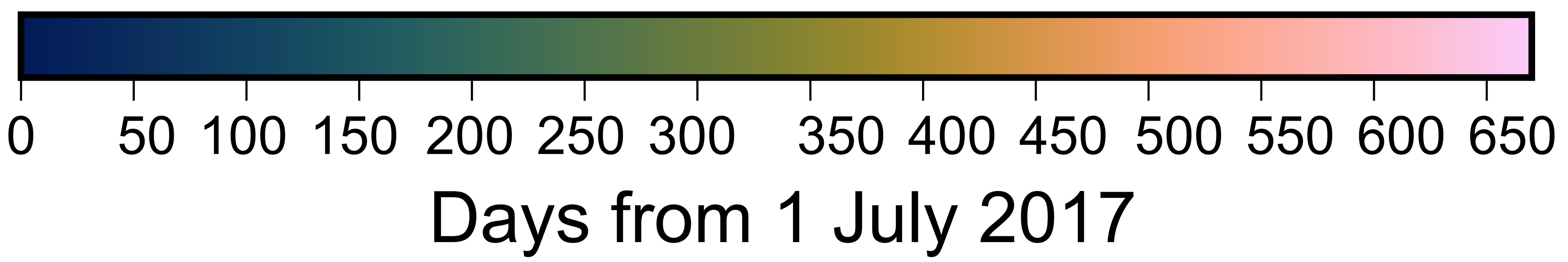

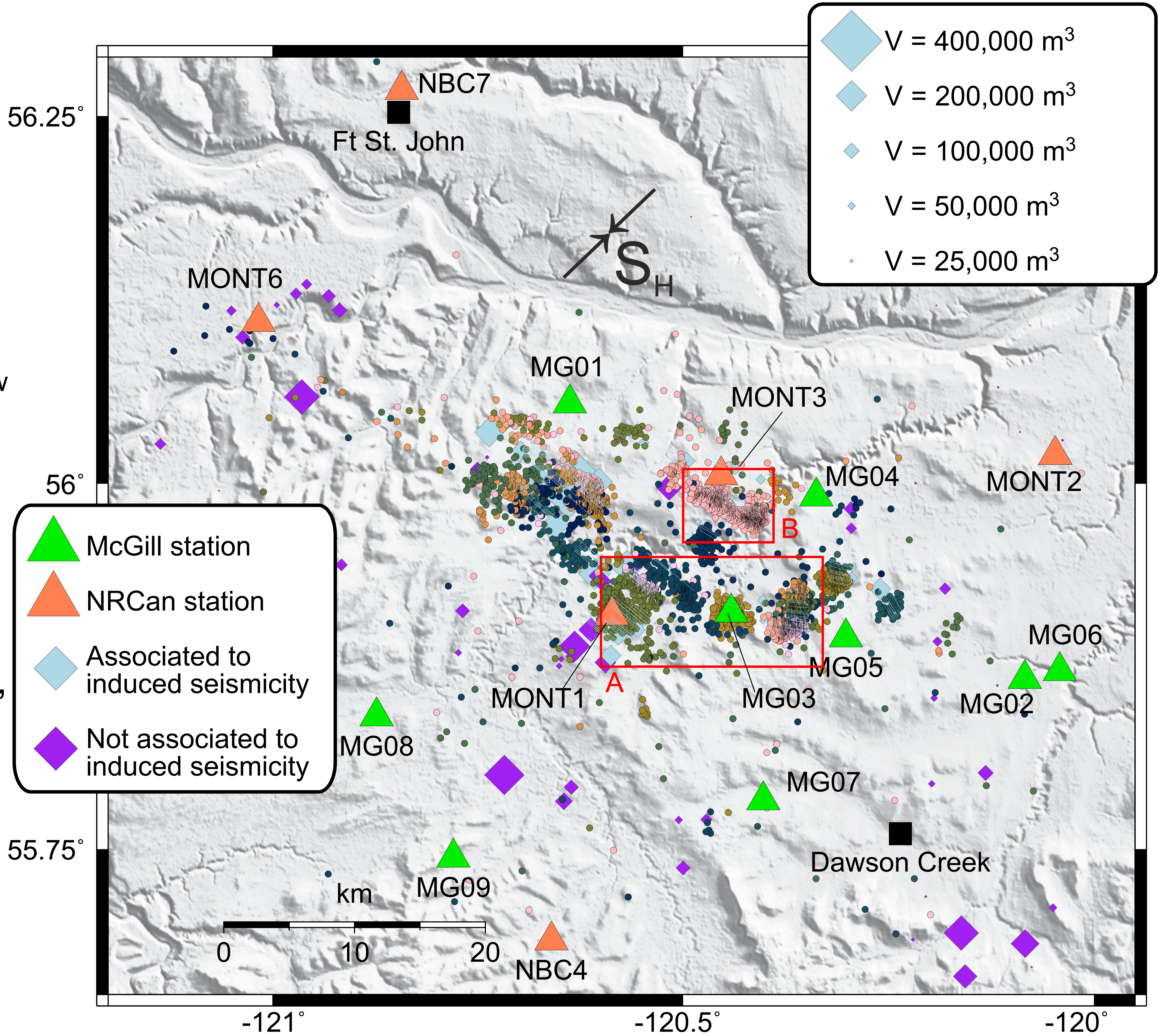

Figure 1a

Methods

Catalog building

- Using continuous waveform data from 15 broadband stations between July 2017 and April 2019, we detect and locate 5757 events (Figure 1a), applying an automated STA/LTA trigger with manually corrected picks, a 1D layered velocity model, as well as NonLinLoc, and SeisComP3.

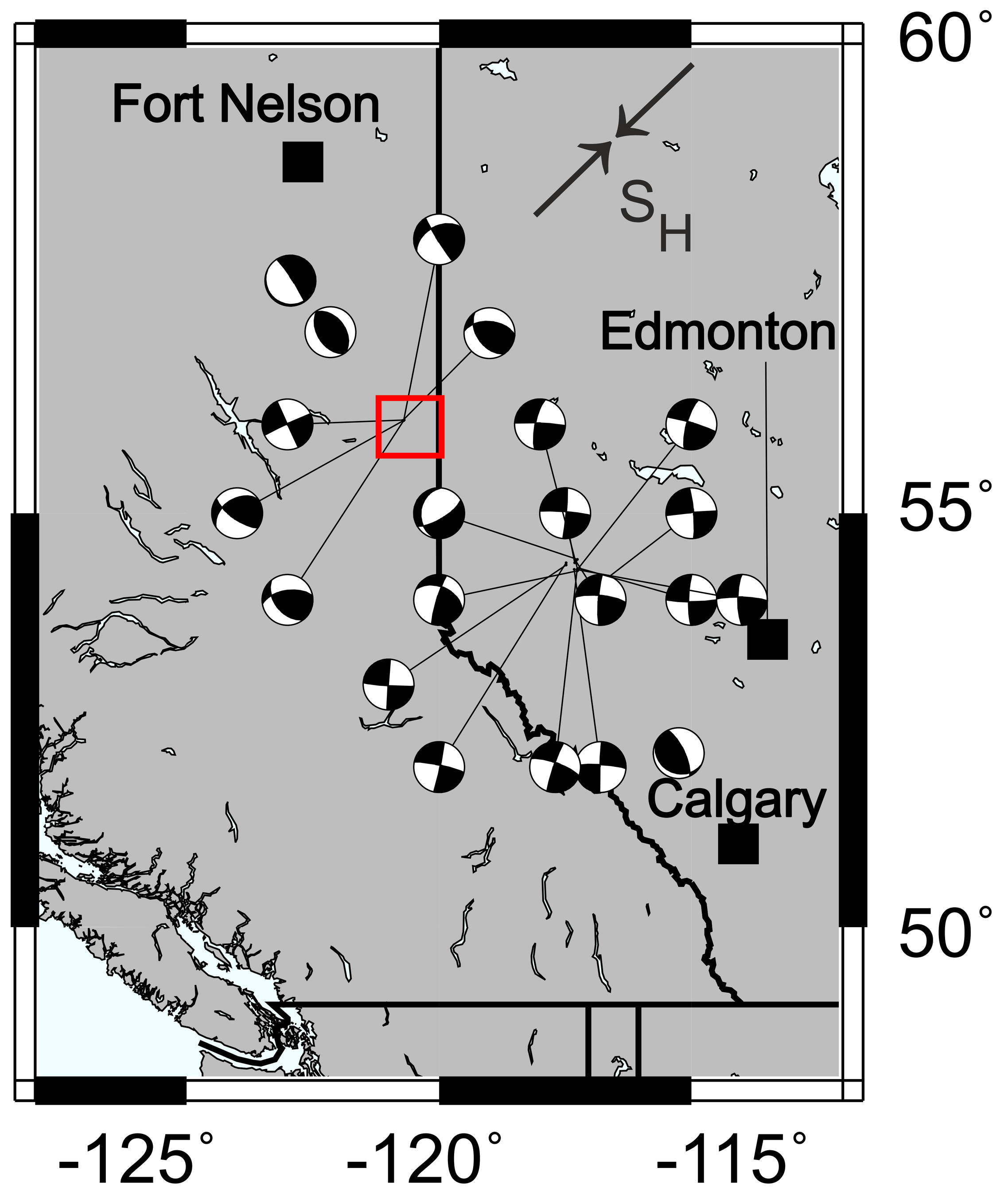

Figure 1b

Regional overview of focal mechanism solutions[1-7] in the WCSB

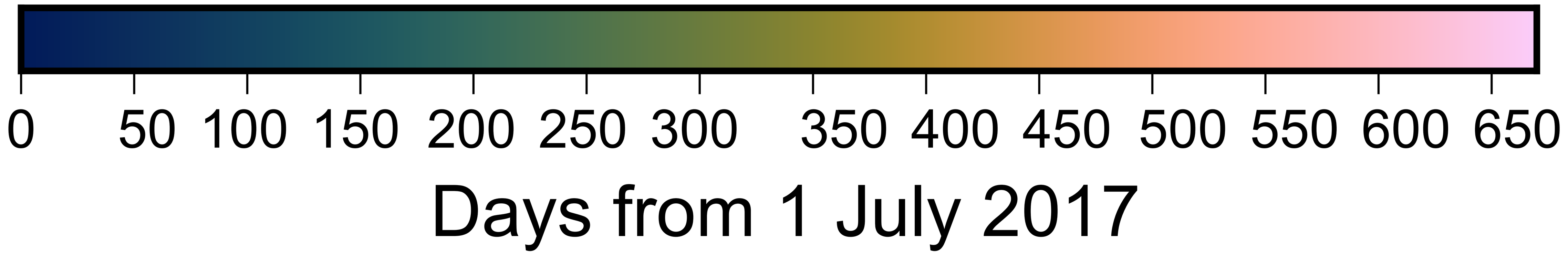

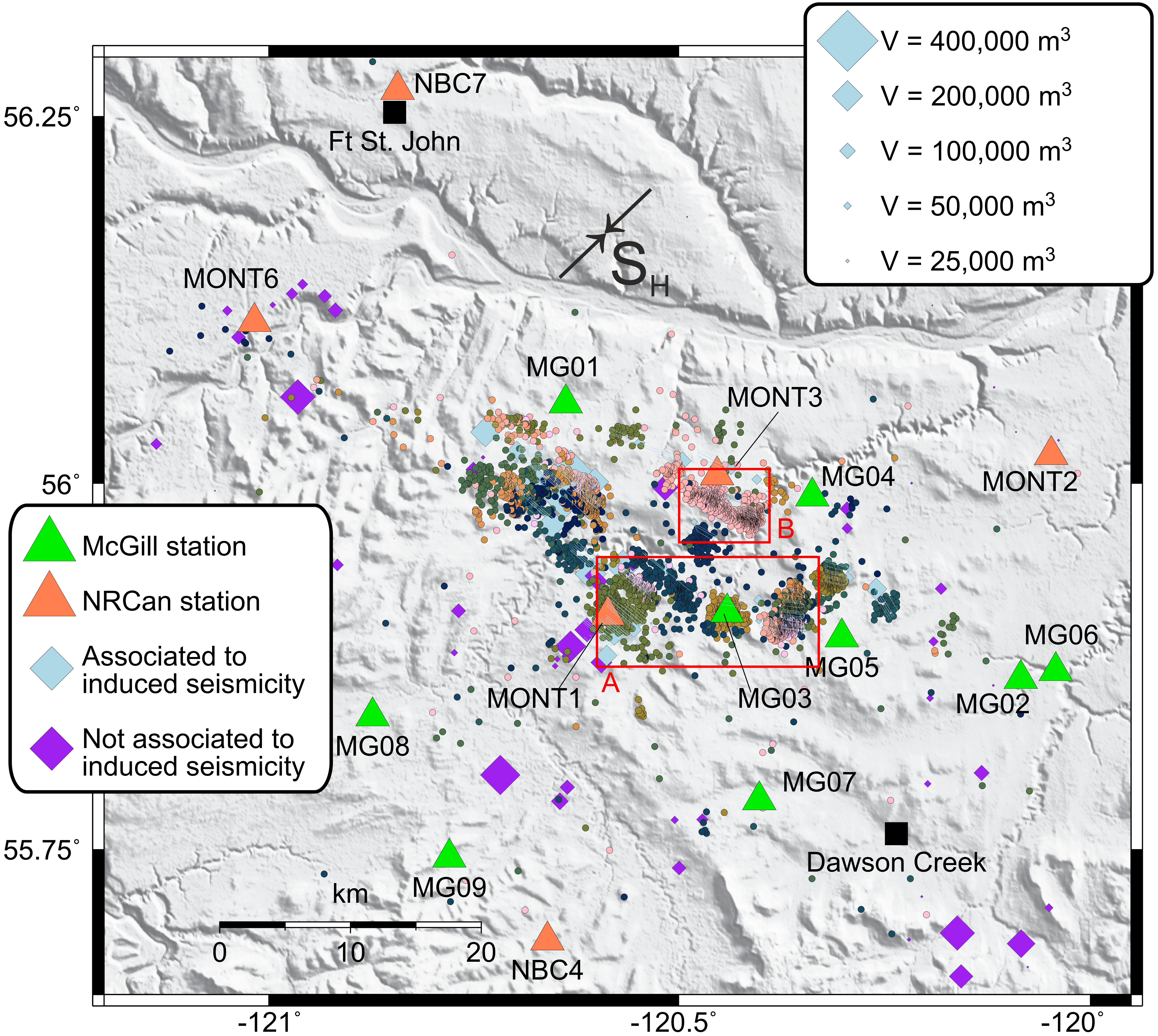

Figure 1a

Methods

Clustering and fluid injection coupling

- Daily earthquakes and seismic moment shows temporal event groups (Figure 2).

- Cross-correlation based similarity analysis applied to create event families (Figure 3; below) and double-difference relocations (Figure 4,5; below).

- Gray shading: periods of injection, with total fluid volume injected in wells within 5 km of an event family shown by the cyan line (Figure 2).

Figure 2

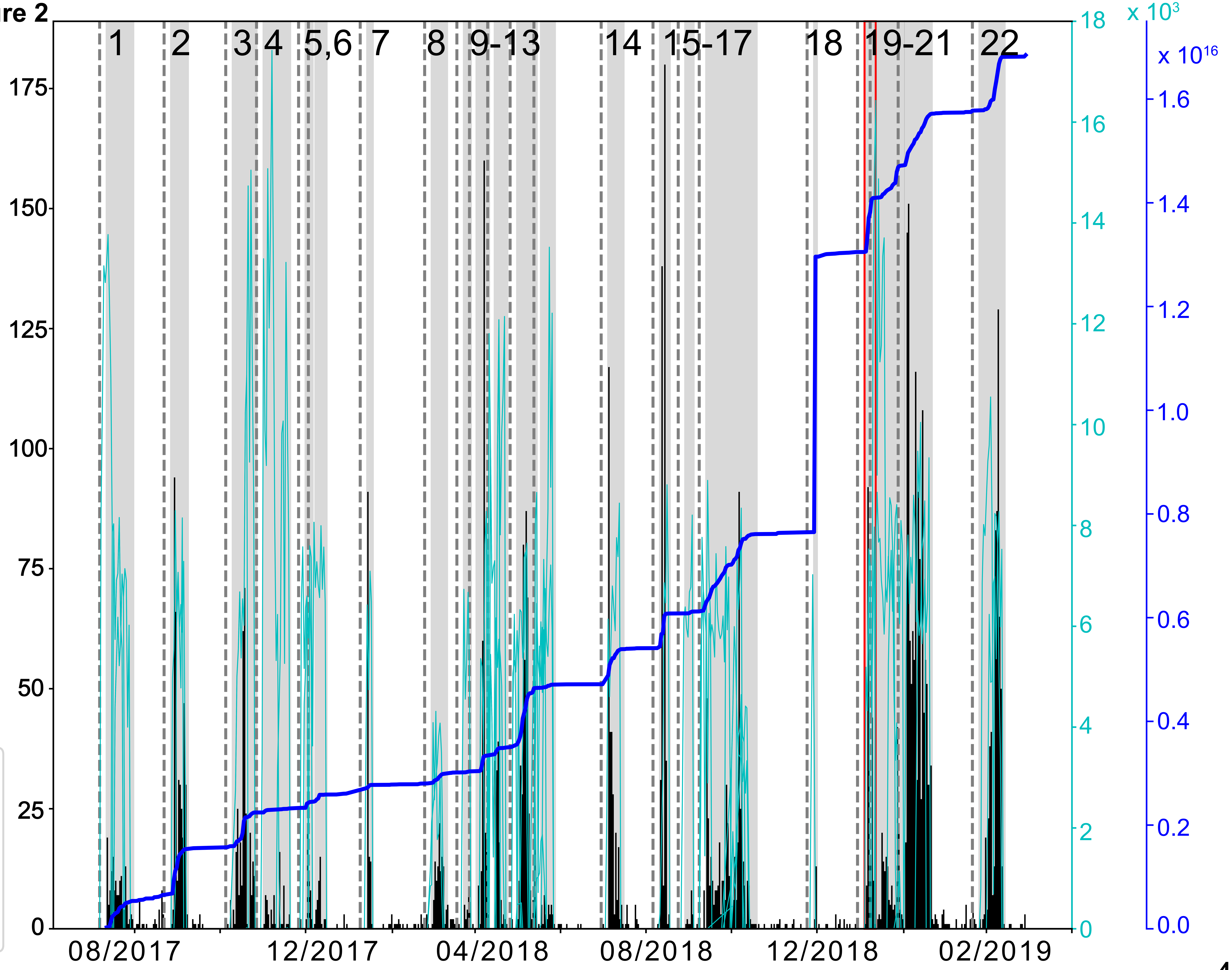

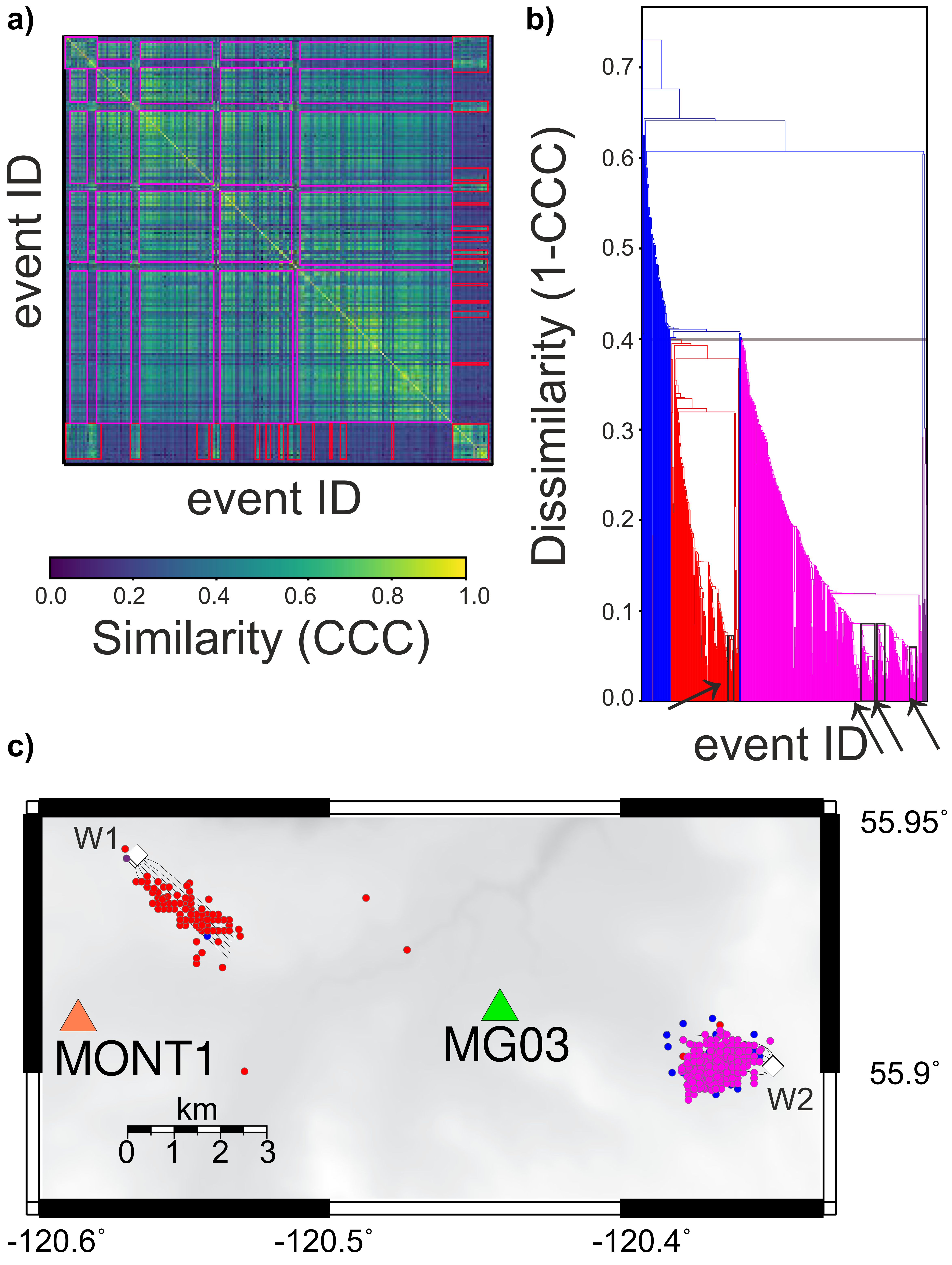

Figure 3

Waveform-similarity based clustering for the time window of March 27th, 2019 to April 13th, 2019. (a) Network similarity matrix, where each pixel indicates CCC for intersecting events (event pairs) indicated on the axes. Colorbar below indicates the CCC. (b) Dendrogram imaging the hierarchical clustering among the events shown in similarity matrix in (a). A threshold CCC > 0.6, or dissimilarity (1 - CCC) < 0.4 (indicated by the grey line) defines earthquake families. Two families are defined in (b) (red and magenta branches), and a number of unassociated events are shown with blue branches. (c) Initial catalog locations of events within the time window, where color coding matches (b) Diamonds indicate the well head location of the active wells in the same period.

Figure 4

Relative relocations of the two event families shown in Figure 3 (red and magenta families, (a) and (b)) in the 22nd time window. The colorbar shows the temporal migration of events (circles) and HF stages (crosses along horizontal well trajectories) in hours following the first HF stage. Relocations show strong lineations trending ENE at low angles to S_H.

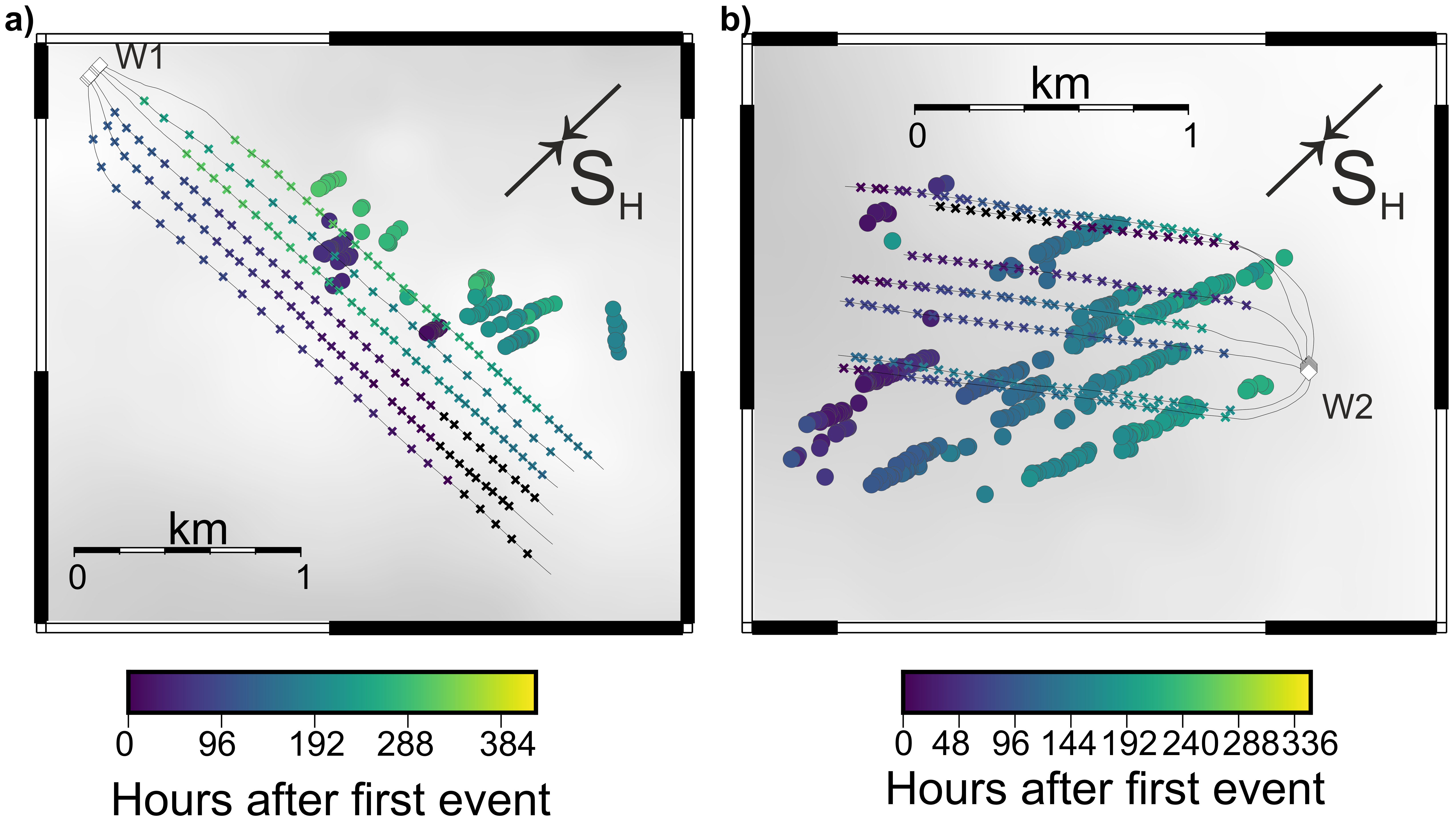

Results

Earthquake catalog

- 5757 detections from 07/2017 - 04/2019
- Catalog completeness of M_c 1.3 and b = 0.92, magnitudes ranging between -0.6 and 4.5

Clustering

- 22 temporal event groups
- 39 event families within the 22 temporal groups
- Earthquakes highly spatially/temporally correlate with HF operations (Figure 6; below)

Relocations

- 4191 earthquakes (Figure 7; below) with relative horizontal/vertical location error of 35 m ± 88 m / 96 m ± 556 m.
- Seismicity distribution implies a lineation subparallel (~ 30°) and perpendicular to S_H, consistent with optimally oriented faults, while hypocenters cluster around and above injection depth (Figure 8; below)

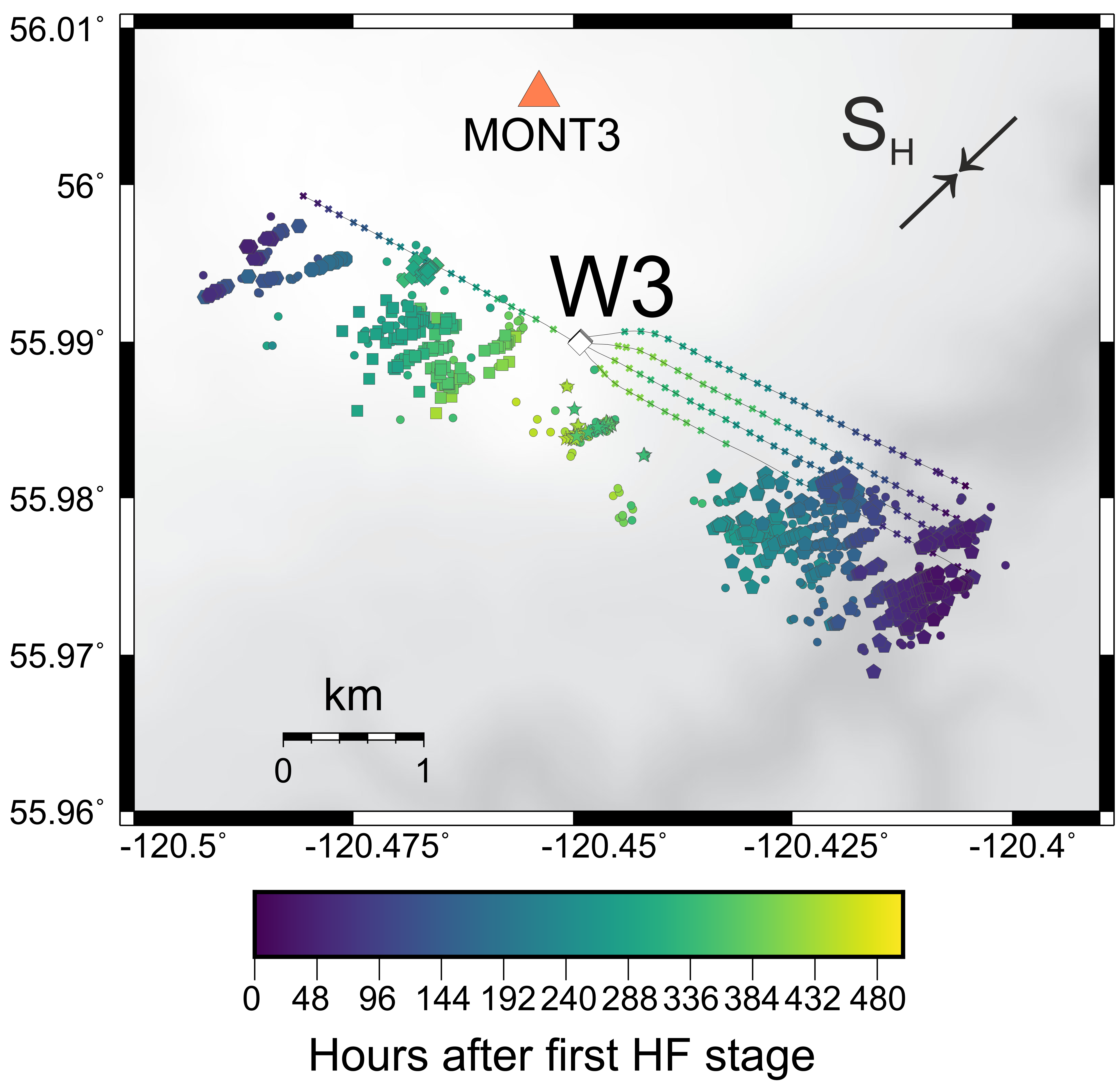

Figure 5

Relative relocations of the event family in time window 21, defined with similarity > 0.7. Colorbar shows temporal migration of events (circles) and HF stages (crosses along horizontal well trajectories) in hours following the first HF stage, and illustrates temporal migration along geological structures suggested by lineations in relocated epicenters. Each symbol group indicates a subfamily with an even higher similarity (≥ 0.82) than the family threshold. In addition to the temporal migration, relocations show the same strong NE-SW lineation as in Figure 4.

Figure 6

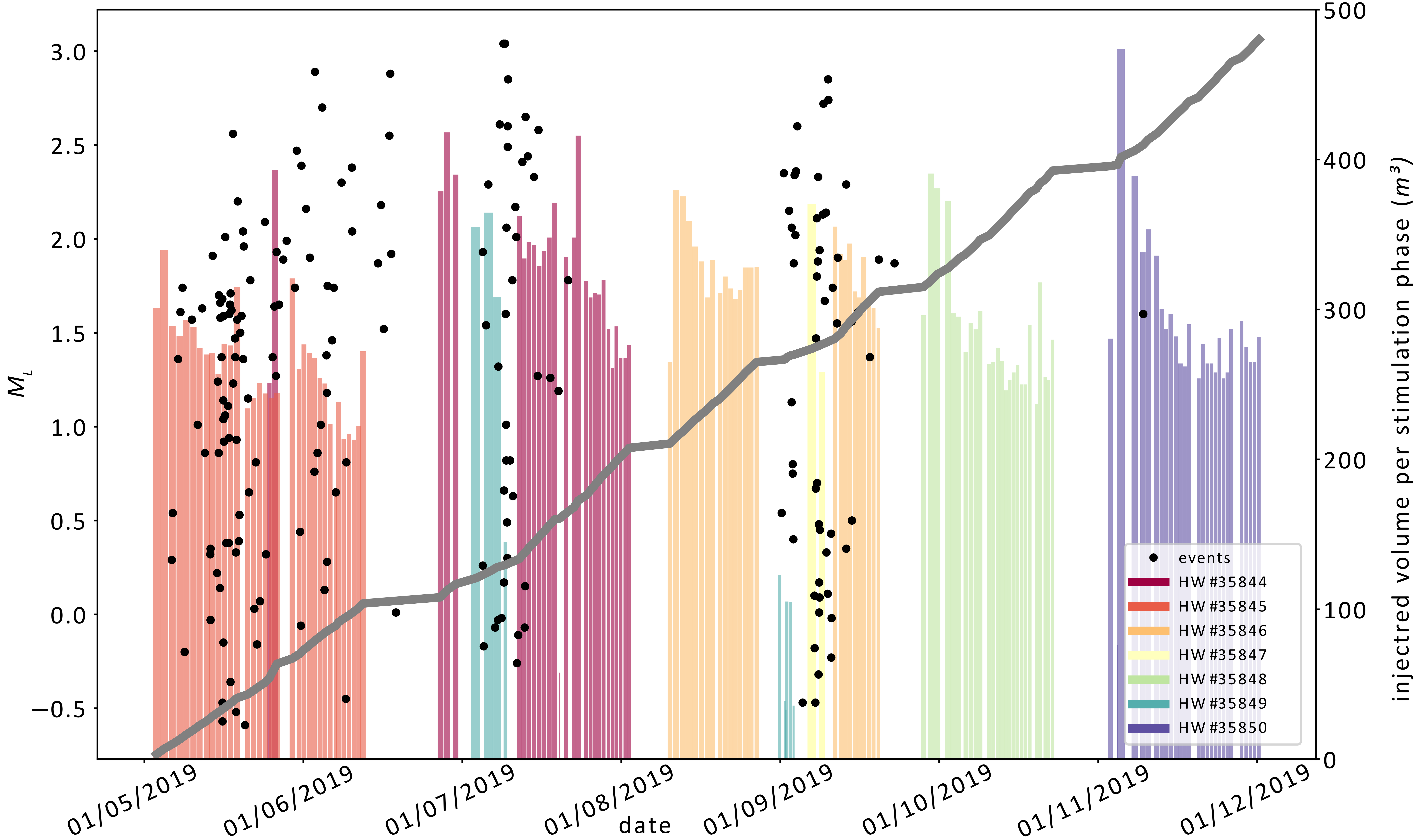

Detailed view of the temporal correlation between seismicity and well stimulation during the time period indicated by the gray shaded area outlined in red in Figure 2. Temporal evolution of injection at individual wells (color coded histogram) and seismicity corresponding to 202 events. A fraction of 81% (163/202) of the earthquakes occur during an ongoing well stimulation. Colored bars show the injected fluid volume per stimulation phase for each horizontal well, and the grey line shows the relative fraction of cumulative injected volume.

Figure 7

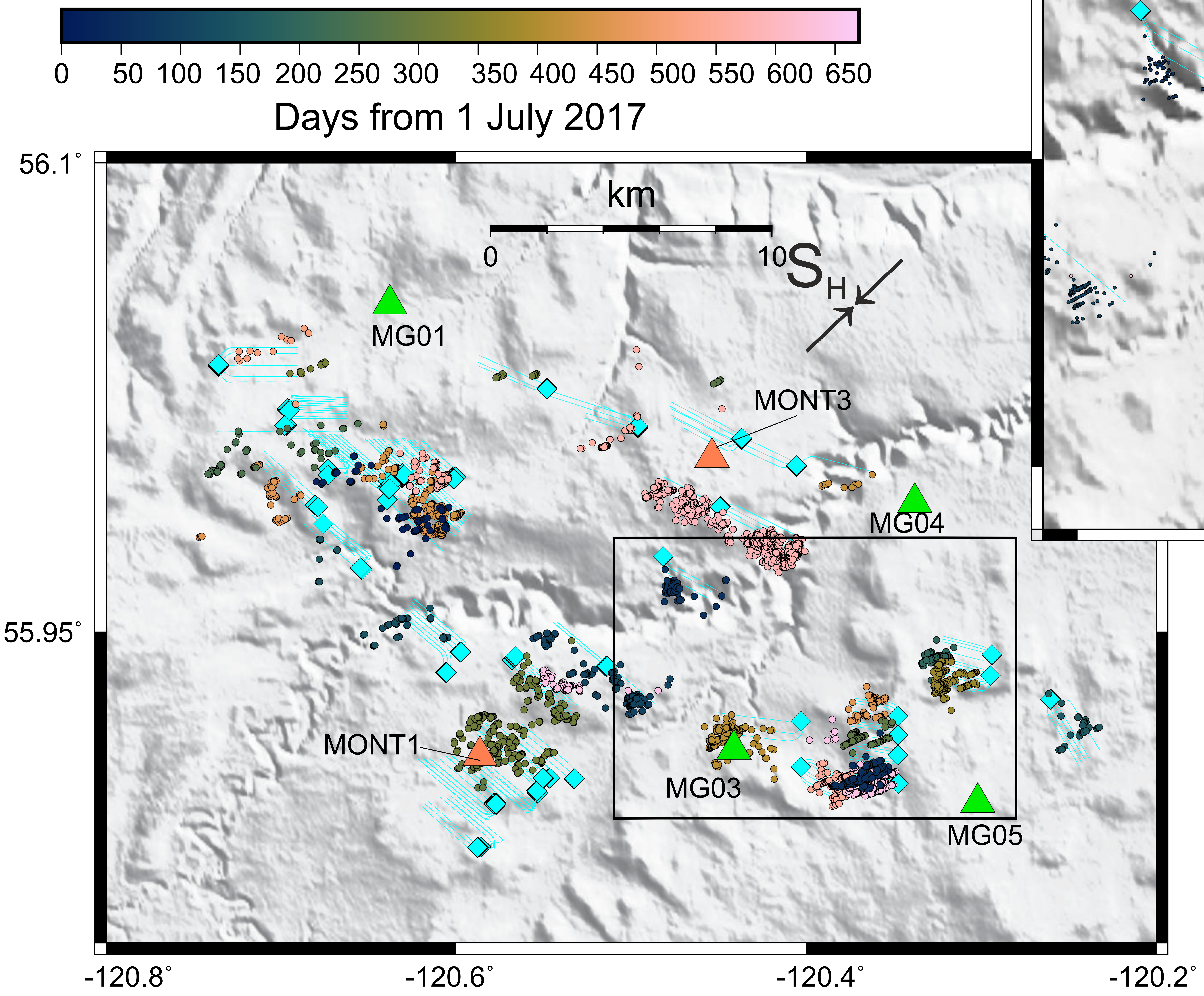

Full scale map of 4191 double-difference event relocations. Colorcode, network, and HF wells are consistent with Figure 1. Inset map highlights the details of lineations in seismicity revealed by the clustered relocation, which includes ENE, and NW trending lineations. The ENE lineations are narrow, suggesting near-vertical dipping faults, where more diffuse NW lineations suggest fault structures with shallower dip angles (relative to vertical).

Figure 8

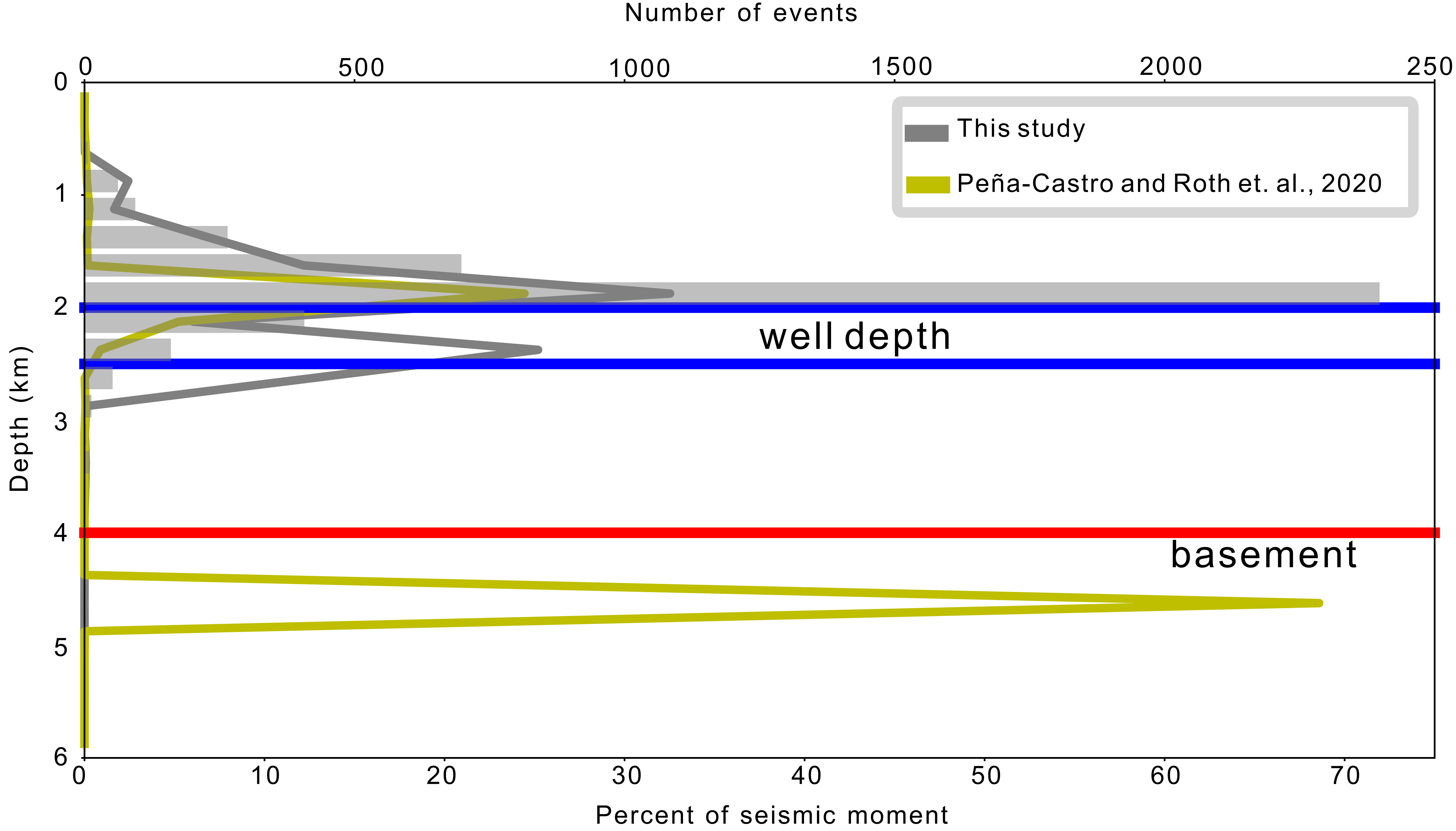

Example of depth distribution with respect to well location. Histogram of the absolute depth distribution of all relocated events, with horizontal bars indicating the well operation depth and the sediment/crystalline basement boundary. Colored lines show the percentage cumulative seismic moment released in 250 m layers for the relocations in this study (grey) and the relocations from Peña-Castro and Roth et al. [2020] (yellow). The difference in hypocentral depths for the November 2018 M_L 4.5 earthquake (corresponding to the jump in cumulative moment at 4.5 km depth) results from a larger number of events in the relocation cluster in the study of Peña-Castro and Roth et al. [2020][7].

Discussion

Possible causes of clustering

- Multiple wells operating in the same time period separated by distances > 5 km (Figure 3)
- Temporal event migration along the dominant direction of horizontal wells (Figure 5)
- Multiple parallel fault structures close to one individual well generate earthquakes (Figure 4)

Possible causes for two dominant observed seismicity lineations

- In the WCSB, two dominant focal mechanisms are observed (Figure 1b), i.e. thrust faulting and strike-slip faulting
- Ambient stress field suggests thrust faulting ($S_H > S_h > S_v$)[8]
- Potentially preexisting fault structures from horst and graben systems[9] or the thrust-fault belt in the Rocky Mountains foreland[10]
- Localized stress changes ($S_H > S_v > S_h$)
- S_h and S_v may be similar in magnitude

Conclusion

- Short temporal/spatial distance to HF activity suggests localized increase in pore pressure is the earthquake generating mechanism
- Lineations perpendicular and at low-angles (~ 30°) to S_H are consistent with thrust and strike-slip deformation, respectively, on optimally oriented faults.
- While strike-slip deformation occurs above HF injection activity in the sedimentary units, the larger thrust-faulting events may be associated with basement faults formed by orogenic tectonics.

Acknowledgements

This project is partially funded by the Deutsche Forschungsgemeinschaft (DFG, German Research Foundation) – project number 428868223, Ruhr University Bochum (RUB) New Faculty startup funds, and Natural Sciences and Engineering Research Council of Canada Strategic Grant STPGP/494141-2016. We acknowledge H. Kao and PGC, G. Langston, J. Onwuemeka and B. Wang from McGill University, for help in seismic station deployment; S. Venables and BCOGC staff for providing well data and logistical support; K.D. Fischer from RUB Seismological Observatory for help in data acquisition and processing; and the analysts (F. Schocke, M. van Lier and H. Lonke, Ruhr University Bochum) for reviewing the automated picks. M. Roth would also like to thank Geoscience BC Graduate Scholarship for partially supporting this work.

References

[1]Schultz, R., Atkinson, G., Eaton, D., Gu, Y., and Kao, H. (2018). Hydraulic fracturing volume is associated with induced earthquake productivity in the Duvernay play.Science, 359(6373):304–308

[2]Eaton, D. W. and Babaie Mahani, A. (2015). Focal mechanisms of some inferred induced earthquakes in Alberta, Canada. Seismological Research Letters, 86(4):1078–1085

[3]Zhang, H., Eaton, D. W., Li, G., Liu, Y., and Harrington, R. M. (2016). Discriminating induced seismicity from natural earthquakes using moment tensors and source spectra.Journal of Geophysical Research: Solid Earth,121(2):972–993

[4]Schultz, R., Wang, R., Gu, Y. J., Haug, K., and Atkinson, G. (2017). A seismological overview of the induced earthquakes in the Duvernay play near Fox Creek, Alberta.Journal of Geophysical Research: Solid Earth,122(1):492–505.

[5]Babaie Mahani, A., Schultz, R., Kao, H., Walker, D., Johnson, J., and Salas, C. (2017). Fluid injection and seismic activity in the northern Montney play, British Columbia, Canada, with special reference to the 17 August 2015 Mw 4.6 induced earthquake. Bulletin of the Seismological Society of America, 107(2):542–552

[6]Wang, R., Gu, Y. J., Schultz, R., and Chen, Y. (2018). Faults and non-double-couple components for induced earthquakes.Geophysical Research Letters. 45(17):8966–8975

[7]Peña-Castro and Roth, Verdecchia, A., Onwuemeka, J., Liu, Y., Harrington, R. M., Zhang, Y., and Kao, H. (2020). Stress chatter on a fracture network reactivated by hydraulic fracturing.Earth and Space Science Open Archive.

[8]Bell, J. S., & Grasby, S. E. (2012). The stress regime of the Western Canadian sedimentary basin. Geofluids, 12(2), 150-165.

[9]Barclay, J. E., Krause, F. F., Campbell, R. I., & Utting, J. (1990). Dynamic casting and growth faulting: Dawson Creek graben complex, Carboniferous-Permian Peace River embayment, western Canada. Bulletin of Canadian Petroleum Geology, 38(1), 115-145.

[10]Pană, D. I., & van der Pluijm, B. A. (2015). Orogenic pulses in the Alberta Rocky Mountains: Radiometric dating of major faults and comparison with the regional tectono-stratigraphic record. Bulletin, 127(3-4), 480-502.